LASER INTERFEROMETER GRAVITATIONAL WAVE OBSERVATORY
- LIGO -
CALIFORNIA INSTITUTE OF TECHNOLOGY
MASSACHUSETTS INSTITUTE OF TECHNOLOGY

July 1, 2009

Adaptive Noise Cancelation First Progress Report

Clara Bennett

Distribution of this document:

LIGO Scientific Collaboration

California Institute of Technology
LIGO Project, MS 18-34
Pasadena, CA 91125
Phone (626) 395-2129
Fax (626) 304-9834
E-mail: info@ligo.caltech.edu

Massachusetts Institute of Technology
LIGO Project, Room NW17-161
Cambridge, MA 02139
Phone (617) 253-4824
Fax (617) 253-7014
E-mail: info@ligo.mit.edu

LIGO Hanford Observatory
Route 10, Mile Marker 2
Richland, WA 99352
Phone (509) 372-8106
Fax (509) 372-8137
E-mail: info@ligo.caltech.edu

LIGO Livingston Observatory
19100 LIGO Lane
Livingston, LA 70754
Phone (225) 686-3100
Fax (225) 686-7189
E-mail: info@ligo.caltech.edu

http://www.ligo.caltech.edu/

1 Introduction

The purpose of this project is to write a code which will be able to adaptively filter out seismic and acoustic noise from the interferometer signal. However, the first couple weeks were devoted to reading about adaptive filtering theory and working on instrumentation.

2 Wiener Filtering [1]

Wiener filters comprise a special class of linear optimum discrete-time filters. As the name suggests, these filters are linear, which makes the mathematics far simpler, and operate in discrete time, allowing for implementation in digital devices. The details of the filter also depend on whether the impulse response is infinite or finite, and the statistical criterion used to optimize the filter.

Infinite response (IIR) filters have feedback loops that feed back to the input, while finite response (FIR) filters utilize only forward paths. The advantage of using FIR filters is their inherent stability–the feedback loops of IIR filters can unwanted oscillations if they are improperly designed. The stability issue for IIR filters is manageable, but if the filter is also required to be *adaptive*–able to track a non-stationary minimum on the error performance surface–the compounded stability problems of adaptive *and* IIR filtration become far too difficult to be practical. For these reasons, the FIR filters (which are, in fact, a special case of IIR) are preferred.

In terms of potential statistical criteria, the choices include minimizing the mean-square of the error estimate, the expectation value of the error, or the expectation third or greater powers of the error. Of these, the first choice is best, as it yields a cost function, J, which is second-order in dependence on the filter coefficients. Thus, J has a distinct and unique minimum, which conveniently provides a single point of optimum filtration.

2.1 A Brief Motivation [1]

To begin, consider a filter input sampled on a discrete time series $u(0), u(1), u(2), \ldots$, and a corresponding filter inpulse response $\omega_0, \omega_1, \omega_2, \ldots$ (assumed to be complex-valued and infinite). The filter output, $y(n)$, at discrete time n, is an estimation of the desired output $d(n)$ [2]. It is given by the linear convolution sum

$$y(n) = \sum_{k=0}^{\infty} \omega_k^* u(n-k), \quad n = 0, 1, 2, \ldots, \tag{1a}$$

[1] For a full derivation, please see Chapter 2 of Reference [1]

[2] Note that the filter input and desired response are both assumed to have a zero mean. In the case of a nonzero mean, it is simply subtracted from the proper quantity before filtering.

with the error being defined as

$$e(n) = d(n) - y(n). \tag{1b}$$

We choose to optimize the filter by minimizing the mean-square of $e(n)$, so

$$J = E[e(n)e^*(n)] = E[|e(n)|^2], \tag{1c}$$

where E is the expectation operator.

Without going into the full details, by assuming (reasonably) that the filter coefficients, ω_k, are complex and requiring that all terms of the gradient of the cost function, ∇J, be zero, one arrives at the following optimization condition:

$$E[u(n-k)e_0^*(n)] = 0, \quad k = 0, 1, 2, \ldots. \tag{2}$$

The minimum of the cost function, naturally, occurs where $\nabla J_k = 0$ for all k. The condition in Eq.(2) implies that, in order for J to be at its minimum value, the corresponding estimation error, $e_0(n)$ must be orthogonal to the input for all times n.

We may substitute Eqs.(1a) and (1b) into Eq.(2) to reconfigure the necessary and sufficient condition of optimization, yielding

$$\sum_{i=0}^{\infty} \omega_{oi} E[u(n-k)u^*(n-i)] = E[u(n-k)d^*(n)], \quad k = 0, 1, 2, \ldots, \tag{3a}$$

where ω_{oi} is the ith optimum filter coefficient. The two expectations in Eq. (3a) are redefined as

$$r(i-k) = E[u(n-k)u^*(n-i)], \tag{3b}$$

$$p(-k) = E[u(n-k)d^*(n)], \tag{3c}$$

where $r(i-k)$ represents the autocorrelation function of the filter output and the cross-correlation of the filter input, $u(n-k)$, and the desired response, $d(n)$, is given by $p(-k)$. Substituting, this brings us to

$$\sum_{i=0}^{\infty} \omega_{oi} r(i-k) = p(-k), \quad k = 0, 1, 2, \ldots, \tag{4}$$

an infinite set known as the Wiener-Hopf equations–the fundamental equation set for Wiener filters.

Up until this point, it was assumed that the impulse response was infinite (IIR). It turns out that, aside from being more practical, the special case of FIR filters simplifies the solution to the Wiener-Hopf equations tremendously. For a filter of length M, the impulse response of the filter is given by the set of tap weights, $\omega_0, \omega_1, \ldots, \omega_{M-1}$ (the coefficients of the filter at each sample, or tap point). Thus, we may reduce the Wiener-Hopf equations to a finite set of M equations

$$\sum_{i=0}^{M-1} \omega_{oi} r(i-k) = p(-k), \quad k = 0,1,2,\ldots,M-1, \tag{5}$$

where the o subscript indicates the optimum value.

The Wiener-Hopf equations may be described as matrices. Consider $\mathbf{R}$ to be an $M \times M$ matrix representing the correlation of the tap inputs of our FIR filter:

$$\mathbf{R} = E[\mathbf{u}(n)\mathbf{u}^H(n)], \tag{6a}$$

where

$$\mathbf{u}(n) = [u(n), u(n-1), \ldots, u(n-M+1)]^T. \tag{6b}$$

Then, $\mathbf{R}$ is expanded into

$$\mathbf{R} = \begin{bmatrix} r(0) & r(1) & \cdots & r(M-1) \\ r^*(1) & r(0) & \cdots & r(M-2) \\ \vdots & \vdots & \ddots & \vdots \\ r^*(M-1) & r^*(M-2) & \cdots & r(0) \end{bmatrix}. \tag{6c}$$

We may also define a cross-correlation vector between the tap inputs and $d(n)$ as follows:

$$\mathbf{p} = E[\mathbf{u}(n)d^*(n)], \tag{7a}$$

which expands to

$$\mathbf{p} = [p(0), p(-1), \ldots, p(1-M)]^T. \tag{7b}$$

This brings us to the matrix formulation of the Wiener-Hopf equations

$$\mathbf{R}\mathbf{w}_o = \mathbf{p} \tag{8}$$

where $\mathbf{w}_o$ is the $M \times 1$ tap-weight vector:

$$\mathbf{w_o} = [\omega_{o0}, \omega_{o1}, \ldots, \omega_{o,M-1}]^T. \tag{9}$$

Rearranging, and assuming the matrix $\mathbf{R}$ to be nonsingular, we find the formula for the optimum filter tap weights to be

$$\mathbf{w}_o = \mathbf{R}^{-1}\mathbf{p}.$$

The eventual purpose of the project will be to create an adaptive Wiener filter to subtract out seismic and acoustic noise, but thus far only the theory has been studied.

3 Mode Cleaner

Before entering into the interferometer, the laser beam is run through a triangular set of mirrors, known as a *mode cleaner*. The optics are suspended on pendula, just like the test masses in the main body of the interferometer. The mode cleaner's purpose is to suppress the non-fundamental modes in the laser beam.

3.1 Fabry-Perot Cavities

A basic Fabry-Perot cavity acts as a "bottle" for laser light (see Figure 1, provided that the cavity is exactly an integer number of wavelengths of the light being stored. It consists of two highly reflective mirrors. A laser beam is pumped in through the first mirror and bounces back off the far end. If the two beams are in phase, they will constructively interfere. Eventually, the trapped light reaches an equilibrium such that the incoming power is equivalent to the power escaping the cavity from scattering, etc.

The LIGO mode cleaner has a triangular structure (see Figure 2), but the basic principle is the same. The cavity is designed to allow only the desired modes of light to resonate, suppressing all others.

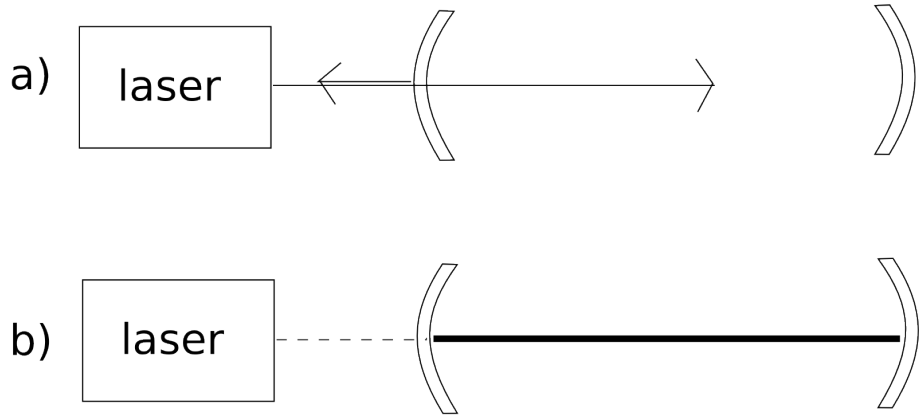

Figure 1: A Fabry-Perot Cavity
a) The laser beam entering the cavity is partially reflected and partially transmitted.
b) If the cavity is the proper length, light will be stored inside, interfering constructively and building up power that is far greater than that of the incoming beam. At equilibrium, the light being transmitted at the first mirror will exactly cancel (destructively interfere) with the incoming beam.

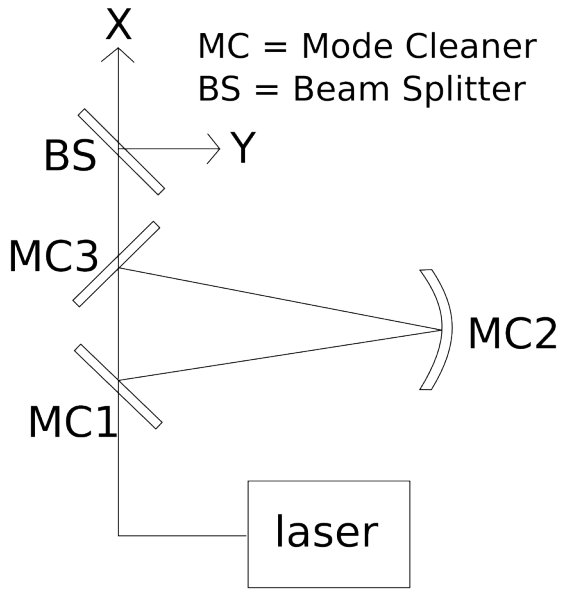

Figure 2: Diagram of the mode cleaner. The laser light continues on from the beam splitter into the X and Y arms of the interferometer. Two sets of three accelerometers each are located at the MC1 and MC2 optical chambers.

3.2 Hermite-Gaussian Modes [2]

There are many transverse amplitude distributions that maintain their forms functionally as they travel. These are known as the Hermite-Gaussian modes, and they are normal modes of diffraction in free space. The modes are composed of Gaussians multiplied by Hermite polynomials in the two directions transverse to propagation, defined as

$$\psi_m(\xi) \equiv H_m(\xi)e^{-\xi^2/2} \tag{11}$$

Recall that the Hermite polynomials represent the quantum mechanical wave function modes for a simple harmonic oscillator potential. Indexing the two polynomials (one for each transverse dimension) as m and n, we obtain the general Hermite-Gaussian mode

$$u_{mn}(x,y,z) = C_m n/\sqrt{1+x^2\lambda^2/\pi^2\omega_0^4}e^{i(m+n+1)\phi}\xi_m(\sqrt{2}y/\omega)\xi_n(\sqrt{2}z/\omega)e^{-ik(y^2+z^2)/2R} \tag{12}$$

Notice that for $m = n = 0$, or the 00 mode, the formula reduces to a pure Gaussian. This is the desired fundamental mode. Also, because the mn mode has a phase factor of $e^{i(m+n+1)\phi}$, modes will have different phases through propagation. So, different modes will resonate for various wavelengths of light, or for different cavity lengths at a fixed wavelength. For a cavity of length L, the resonant wavelengths are

$$\lambda_{mnp} = 2L[p+2(m+n+1)/\pi tan^{-1}L\lambda/2\pi\omega_0^2]^-1, \tag{13}$$

where the p index indicates the number of wavelengths along the length of the resonating cavity.

By taking advantage of these phase differences, it is possible to set up a Fabry-Perot cavity that will resonate for only the desired mode(s) and suppress all others, thus "cleaning" the mode of laser beam. For the purposes of the LIGO interferometer, the mode cleaner is set up to isolate the purely Gaussian mode (00).

4 Instrument Position Optimization

Currently, there is a set of three accelerometers, one for each dimension, located at both the first and second mode cleaner optics (MC1 and MC2). There is also a three-dimensional Guralp seismometer near MC1 and a Ranger seismometer measuring in the y-direction at MC2. We are trying to optimize the positioning of these instruments in order to get the best Wiener filtering results. At this time, only the accelerometers have been adjusted.

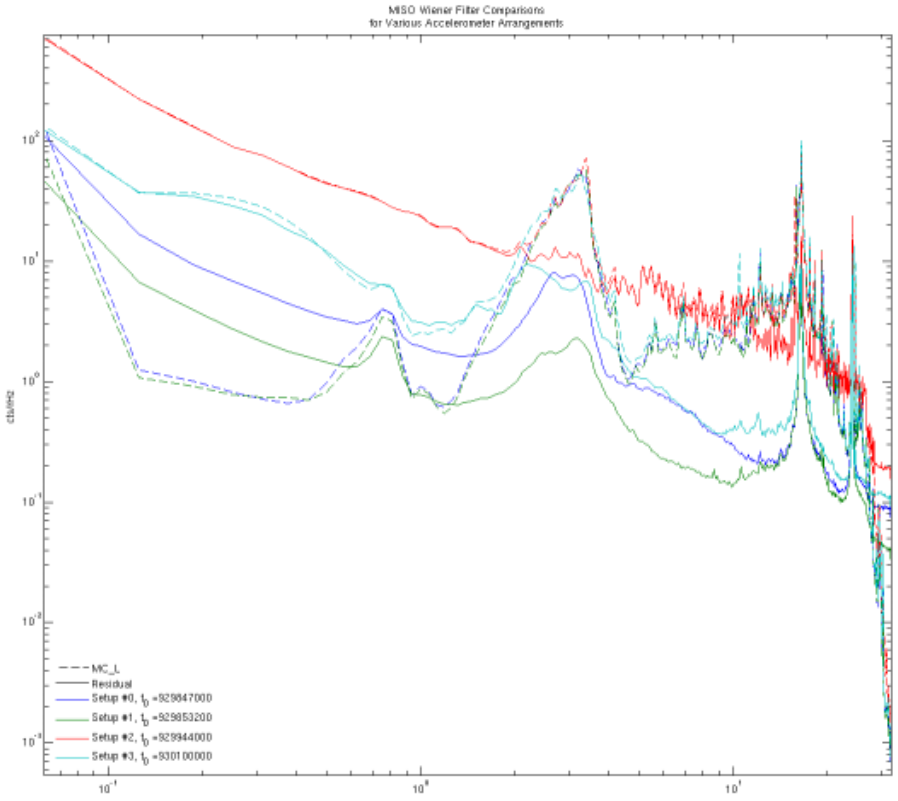

Figure 3: Plot of Wiener-filtered noise for each arrangement of the accelerometers. See Figures 5 and 6 for positioning for each setup number.

4.1 Accelerometers

Several different arrangements of the accelerometers were tried. Figure 3 shows how well the existing Wiener filter could remove noise based on these configurations (for the actual positions of the setups, see Figures 5 and 6), using data over 80-minute intervals. Setup 1 seems to be the best, but the accelerometers were not left in that position for very long, so we cannot compare over longer intervals. They have been returned to Setup 1 to verify the results.

5 Microphones

While the 40m laboratory does currently have accelerometers and seismometers set up to measure seismic noise sources, it has only a single, low-quality microphone that is too noisy to be useful. Two condenser microphones were purchased to provide better measurements of acoustic noise sources. Condenser microphones are popular in laboratory applications due to the comparatively small mass that must be moved by the incoming sound waves, requiring the sound waves to do less

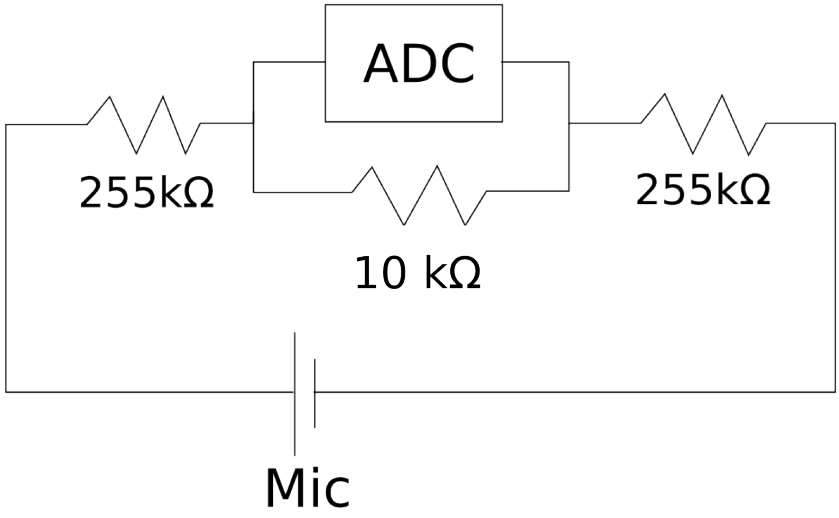

Figure 4: Voltage divider design.

work. The particular model purchased covers the 20Hz - 20kHz frequency range.

Due to the size of the lab, the required cables were longer than could be found ready-made. So, two 80-ft XLR cables were made for that purpose. Also, the Analog-to-Digital Converter (ADC) can only handle about $\pm$2V. Crude sound-testing of the microphone - preamplifier setup showed that, even on the lowest gain setting, the voltage output could reach $\pm$6V. However, due to the length of the cables, it would be advantageous to be able to operate the preamplifier with a high gain setting, with which we were able to create voltage outputs of about $\pm$70V. Voltage dividers were designed so that, even with an input of $\pm$100V, the ADC would not be overloaded (see Figure 4).

References

[1] Haykin, Simon. *Adaptive Filter Theory–4th Edition.* Prentice Hall. New Jersey: 2002.

[2] Saulson, Peter R. *Fundamentals of Interferometric Gravitational Wave Detectors.* World Scientific Publishing. New Jersey: 1994.

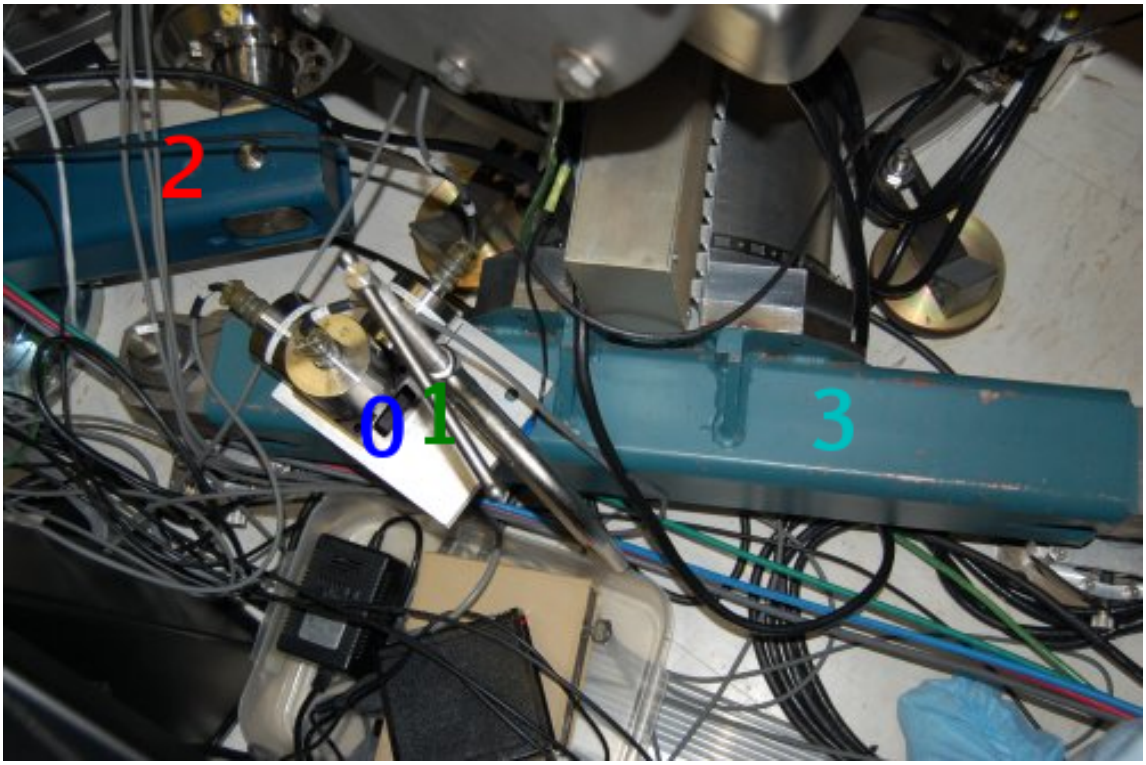

Figure 5: Positions of the MC1 accelerometer set for each setup. The accelerometers are pictured in the Setups 0 and 1 position.

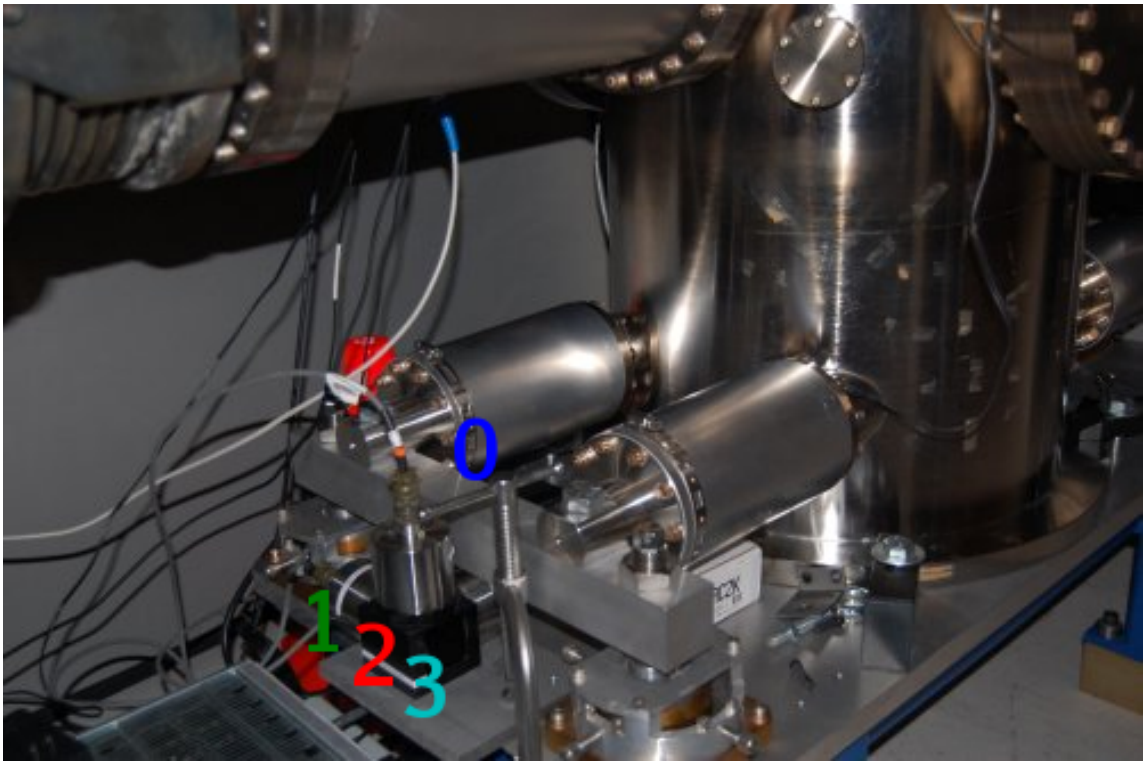

Figure 6: Positions of the MC2 accelerometer set for each setup. The accelerometers are pictured in the Setups 1, 2, and 3 position.